

Evaluation of Bearing Capacity of Strip Foundation Subjected to Eccentric Inclined Loads Using Finite Element Method

Ahmed Majeed Ali

Assistant Lecturer

Building and Construction Engineering Department, University of Technology/ Baghdad

Ama.civil85@gmail.com

ABSTRACT

In real conditions of structures, foundations like retaining walls, industrial machines and platforms in offshore areas are commonly subjected to eccentrically inclined loads. This type of loading significantly affects the overall stability of shallow foundations due to exposing the foundation into two components of loads (horizontal and vertical) and consequently reduces the bearing capacity. Based on a numerical analysis performed using finite element software (Plaxis 3D Foundation), the behavior of model strip foundation rested on dry sand under the effect of eccentric inclined loads with different embedment ratios (D/B) ranging from (0-1) has been explored. The results display that, the bearing capacity of strip foundation is noticeably decreased with the increase of inclination angle (α) and eccentricity ratio (e/B). As well as, a reduction factor (RF) expression was appointed to measure the degree of decreasing in the bearing capacity when the model footing is subjected to eccentric inclined load. It was observed that, the (RF) decreases as the embedment ratio increases. Moreover, the test results also exhibit that, the model footing bearing capacity is reduced by about (69%) when the load inclination is varied from (0° to 20°) and the model footing is on the surface. While, the rate of decreasing in the bearing capacity was found to be (58%), for both cases of footing when they are at embedment ratios of (0.5 and 1.0). Also, a comparative study was carried out between the present results and previous experimental test results under the same conditions (soil properties and boundary condition). A good agreement was obtained between the predicted bearing capacities for the two related studies.

Keywords: strip foundation, inclined loads, eccentricity ratio, finite element method.

تقييم قابلية تحمل الأساس الشريطي المعرض لأحمال مائلة غير مركزية باستخدام طريقة العناصر المحددة

احمد مجيد علي

مدرس مساعد

قسم هندسة البناء والإنشاءات، الجامعة التكنولوجية/ بغداد

الخلاصة

في الظروف الحقيقية لأسس المنشآت مثل الجدران الساندة، المكاين الصناعية و منصات في مناطق بحرية تكون معرضة إلى أحمال مائلة بشكل غير مركزي. هذا النوع من التحميل يؤثر بشكل مهم على كامل إستقرارية الأسس الضحلة نتيجة تعرض الأساس إلى مركبتين من الأحمال (أفقية وعمودية) وبالتالي تقلل من قابلية التحمل. اعتماداً على تحليل عددي أنجز باستخدام برنامج يعتمد على طريقة العناصر المحددة (Plaxis 3D Foundation)، فإن تصرف نموذج الأساس الشريطي المستند على رمل جاف و تحت تأثير أحمال مائلة غير مركزية وبنسب غرز (D/B) مختلفة تتراوح من (0-1) قد تم التحري عنه. تظهر النتائج بأن قابلية تحمل الأساس الشريطي تقل بشكل ملحوظ بزيادة زاوية الميلان و نسبة اللامركزية. أيضاً مصطلح معامل التقليل قد اعتمد لقياس درجة النقصان في قابلية التحمل أثناء تعرض الأساس إلى حمل مائل غير مركزي. وقد لوحظ إن معامل التقليل يقل عندما تزداد نسبة الغرز. علاوة على ذلك، تظهر نتائج الفحوصات بأن قابلية تحمل نموذج الأساس يقل بنسبة حوالي (69%) عندما يتغير ميلان الحمل من (0-20°) ونموذج الأساس يكون على السطح. بينما، وُجد أن نسبة النقصان في قابلية التحمل هي (58%) وذلك لكلا الحالتين والذي عندما يكون فيها الأساس عند نسب غرز (0.5-1.0).

أنجزت دراسة مقارنة بين النتائج الحالية ونتائج فحوصات مختبرية سابقة تحت نفس الظروف (خواص التربة, حالة الحدود). تم الحصول على توافق جيد بين قابليات التحمل المخمنة للدراستين المقصودتين.
الكلمات الرئيسية: أساس شريطي, احمال مائلة, نسبة اللامركزية, طريقة العناصر المحددة

1. INTRODUCTION

Based on the review of the existing literatures related to the bearing capacity of shallow foundations, it seems a limited attention has been paid to predict the ultimate bearing capacity when the foundation is subjected to eccentric and inclined loads. Hence, the paucity of the numerical and experimental studies concerning the eccentrically inclined loads gives the impulsion to carry out numerous researches in this field.

However, loads on footings are normally eccentric and inclined, as shown in **Fig 1**. Loading a footing eccentrically will reduce the bearing capacity of the footing. An off-center load will increase the stress (edge stress) on one side and decrease it on the opposite side. **Purkayastha and Char, 1977** analyzed the method of the stability of slip surfaces that used for computing the bearing capacity of eccentrically loaded footing. A close agreement was noticed between the theoretical and experimental values for the plane strain case.

Saran and Agarwal, 1991 theoretically assessed the bearing capacity of strip footing under eccentricity and inclined loads. The derived equation from that analysis is expressed as:

$$q_{(e/B, \alpha)} = D \gamma N_{q(e/B, \alpha)} + 1/2 B \gamma N_{\gamma(e/B, \alpha)} \quad (1)$$

Where

$N_{q(e/B, \alpha)}$ and $N_{\gamma(e/B, \alpha)}$ are the bearing capacity factors which are in terms of inclination angle (α) and eccentricity load (e). They are available in tubular and graphical form in the original paper.

Gottardi and Butterfield, 1993 used an alternative approach using "interaction diagram" to relate different loading components at failure for strip footing subjected to eccentrically inclined load on sand. They revealed that, the sign of the eccentricity is important in relation to the direction of the horizontal load.

Loukidis et.al, 2008 employed the finite element method to determine collapse load of a rigid strip footing placed on a uniform layer of purely frictional soil subjected to inclined and eccentric loading. Two series of analyses were performed, one using an associated flow rule and the other using a non-associated flow rule. The results showed that, the inclination factor depends on the value of the friction angle, whereas the effective width (B') does not. Also, laboratory model tests were carried out by **Pritam Dhar et.al, 2013** to investigate the load-inclined and eccentric load under different shapes of model footing.

2. FINITE ELEMENT ANALYSIS AND MESH DESICRETIZATION

A numerical analysis using (Plaxis 3D Foundation) software has been employed to separately characterize the load- settlement relationships of model strip footing. Geometry of mesh generated has planer dimensions of 0.5m (width), 1m (long) and 0.65m in depth. The model foundation dimensions are (500mm) in length and (100mm) in width and has a thickness of (30mm), simulated as mild rigid steel material. The type of soil element used is 15-nodes wedge element, composed of 6- triangular nodes in horizontal direction; and 8- quadrilateral nodes in vertical direction.

The mesh modeled in this case consists of (4026 and 1316) for number of nodes and elements respectively. The choice of 15-noded wedge element was made because the later demonstrates a higher rate of convergence and superior numerical performance than the other types of nodes (i.e. 6

node elements) especially for the dense sand where the intense of strain localization exists, **Loukidis et.al, 2008**. Layout of mesh geometry at different positions of footing is illustrated in **Fig. 2**.

Plaxis automatically imposes a set of general fixities to the boundaries of geometry model. These conditions are generated according to the following rules:

Vertical model boundaries with their normal to x-direction (parallel to y-z directions) are fixed in x-direction and free in y and z directions. Also, vertical model boundaries with their normal in z-direction are fixed in that direction and free in xy plane. While model boundaries neither in x- nor in z- direction are fixed in x and z- direction (displacements in these direction equal to zero) and free in y- direction. The model boundaries for bottom and ground surface are fixed and free respectively in the all directions.

To get a better representation of the interaction between the soil and the foundation, reduction factor R_{int} was used as a value of (0.8). The soil mechanical behavior is modeled using an elastic – perfectly plastic constitutive model following the Mohr– Coulomb failure criterion. Since all the calculations are based on the main input parameters; stiffness and shear strength materials, it can be emphasized in **Table 1**.

2.1 Definition of Problem to be analyzed

This research is concerned with the study of the bearing capacity of a model strip footing of width B, supported by dense sand and located at different depths (D_f/B i.e. 0, 0.5 and 1) at and below the ground level, under the action of eccentric inclined loads. The effect of inclination angles which are varied from ($\alpha=0, 5, 10, 15$ to 20). Eccentricity ratio (e/B) was chosen as (0, 0.05, 0.1 and 0.15) to satisfy the safe design criterion ($e < B/6$) so as to avoid tension between the foundation and soil. All soil properties and foundation details used and the boundary condition in this study have been adopted from **Atalar et.al, 2013**.

3. COMPARATIVE STDY WITH PREVIOUS EXPERIMENTAL RESULTS

Since, the present study has employed the same boundary conditions and the soil properties that were used by **Atalar et.al. 2013** but, the objective is extremely different. So, the comparison between the present numerical test results and the experimental ones in the form of ultimate bearing capacity has been done and listed in Table 2. In most cases, the deviations as demonstrated in col. (3) are less than ± 15 . The summation of these deviations value was about (7.65%), which is mean the degree of convergence between the numerical and experimental results is (92.35%) and provided an excellent agreement in estimating the ultimate bearing capacity of model strip footing subjected to eccentrically inclined load. The correlation between the previous experimental work and the present numerical is better clarified in **Fig.3**.

4. ANALYSIS AND DISCISSION OF TEST RESULTS

Bearing capacity of model strip footings for all tests conducted in this study has been obtained. The coupled effect of combined loads and the eccentricity on the behavior of footing was clarified. As well as, the mechanism of failure under different conditions of loading has also been implied. The criterion adopted in this study is that proposed by **Terzaghi, 1943** by which the failure load is defined as the load required to cause a settlement corresponding to 10% of footing width.

4.1 Effect of Load Eccentricity

Obviously when the load is directly applied at the center of footing, it will be subjected to a vertical displacement almost equal at each point below the footing (i.e. footing is rigid). **Fig. 4** represents the relationship between the pressure and settlement for centrally loaded footing at different embedment ratio (D_f/B).

As shown in **Fig. 4**, it can be observed that, as the eccentricity ratio increases the bearing capacity of model footing to sustain the imposed loads decreases. This issue is true for all off-centrally loaded footing, at which the model footing is confronted to rotating moment about the edge. The model footing will tilt toward the side of the eccentricity and the contact pressure increases on the side of tilt and decreases on the opposite side. As though the failure resulted in the supporting soil on the side at which the load is acted. The ultimate capacities of model footings for different cases are presented in **Fig.5**.

It is noticed that, and according to the loading curves explained above, the type of failure is general shear failure even for the tests carried out at off-central loading. This observation is compatible with **Murthy, 2002** who stated that if the eccentricity is small ($e < B/6$), the load required to produce this type of failure is almost equal to the load desired for producing a symmetrical general shear failure. However, the moment counteracted about the foundation has a direct proportion with the eccentricity value and its effect is listed in **Fig. 6**.

Clearly, the values of moment that work against rotating action is increased as the distance from the center of gravity of foundation is increased. Since, the mobilized moment which tries to prevent the footing to topple is a function of vertical component of inclined load (i.e. $M = v \cdot e$) thus, it is deduced that, the increase in moment when the model footing was placed at embedment ratio of (0.5 to 1) at eccentricity ratio of (0.15) was (80 and 136%) respectively in the comparison with the case of surface footing ($D_f/B = 0$).

This condition is justified to the fact that, installing the footing at a nominated depth and restricted by surrounding soil and which the footing will be resisted by the passive forces exerted by soil bounded the footing. Therefore, presence of the soil at the both sides of footing causes to intensify the passive region which in turn push against the active region below the footing directly and consequently, the footing will contain more external loads, than of the case when the model footing is placed on the surface. **Fig. 7** is presented to understand the failure mechanism and what happens when the model footing is loaded by a vertical eccentric loading ($e > 0$ and $\alpha = 0$).

According to **Bransby and Randolph, 1998** the collapse mechanism when the footing is loaded by off-center vertical load consists of wedge and rotation parts. The wedge has two components: a passive wedge and a fan region. The wedge part lies to the side of footing, on the side upon which the load is applied. Plastic shearing occurs in side of the fan and the passive wedge. In contrast, the plastic strains in the rotation part located on the other side of mechanism tends to occur along the single shear band bounding the rotating part, with only minimal plastic deformations developing inside the rotating part.

4.2 Effect of Load Inclination

Exactly (15) model tests were conducted to investigate the influence of centrally inclined loads ($e/B=0$) at different inclination angles (α) changing from ($0^\circ, 5^\circ, 10^\circ, 15^\circ$ to 20°) and embedment ratio ($D_f/B = 0, 0.5$ and 1.0). The effects of these parameters on the values of bearing capacity are shown in **Fig. 8**. As was expected, the maximum value of load that the model footing can be reached is at the case of (i.e. $\alpha=0$). It is noticed that, the ultimate bearing capacity decreases as the inclination angle increases.

The test results also exhibited the model footing bearing capacity is minimized by about (69%) when the load inclination is varied from (0° to 20°) and the model footing is on the surface. However, the rate of decreasing in the bearing capacity was recorded as (58%), for the both cases of footing when they are at embedment ratios of (0.5 and 1.0). From the findings mentioned above, it is

observed that, the bearing capacity of footing is affected with the embedment ratio in addition to the inclination angle. This justification is attributed to the fact that, the amount of reduce in the bearing capacity of surface footing is larger than that of the cases when the model footing is installed at deeper distance ($D_f/B > 0$).

Normally, the surface footing that subjected to inclined load will be exposed into two components of loads, vertical and horizontal forces. The vertical component is already checked for the bearing capacity purposes. As for the horizontal force, the model footing will be subjected to sliding effect, causing to reduce of entire stability of footing. Since the footing on the surface is free and unbounded from all the direction of the planer area, the horizontal resistance is a function of vertical load according to the expression ($H = V \tan \delta$), meaning that horizontal force is mainly dependent on the friction between the soil and the foundation and the vertical component of loading.

When the model footing is constructed at a certain depth into the ground, the model footing will be confined by the surrounding soil, and the footing will be considerably withstand against sliding action. This may refer to the presence of passive forces exerted on the footing base resulting from the adjacent soil. Therefore, the horizontal force beneath the footing base can be formulated as shown:

$$H = V \tan \delta + P_p \quad (2)$$

Where the (H) is the horizontal resistance of footing, (V) is the vertical component of loading, (δ) is a coefficient of friction and (P_p) is the passive force exerted on the footing which depends upon the friction angle (ϕ) and the soil density (γ). For these reasons, it may be said that, the sliding action is started to minimize as the embedment ratio increases.

In the case of central inclined loading ($e = 0$, $\alpha > 0$) as shown in **Fig. 9**, there is no rotation part in the failure mechanism, which is largely one-sided containing a passive wedge, fan and a rigid tapered wedge below the footing base that pushes against the fan region. A very small passive wedge is observed on the side of mechanism opposite the side of footing where the inclined load points.

4.3 Effect of Eccentrically Inclined Load on Bearing Capacity

In this section, the combined effect of the inclination angle and eccentricity ratio at different embedment ratios was together analyzed. A total of 31 model tests were performed (with regardless of the cases of eccentric and inclined vertical loading which have been mentioned before) for identifying the coupled influence of eccentrically inclined load on the behavior of bearing capacity of model strip footing. The influence of these factors is illustrated in **Fig. 10**.

As seen in these plots, the bearing capacity of footing has an inverse proportion with the eccentricity ratio and the angle of inclination. This principle is consistent for all the values of embedment ratio. The complicated interaction between these parameters is required using reduction factor concept. The term "RF" is used to express and compare the test data from different loading condition. So, the change in the term of bearing capacity is expressed and displayed as the following:

$$RF = 1 - \frac{q\left(\frac{D_f}{B}, \frac{e}{B}, \alpha\right)}{q\left(D_f/B, e/B=0, \alpha=0\right)} \quad (3)$$

Where RF is reduction factor, $q\left(D_f/B, e/B, \alpha\right)$ is the ultimate bearing capacity of footing with different values of eccentricity ratio and the angle of inclination at a specific embedment ratio, $q\left(D_f/B, e/B=0, \alpha=0\right)$



is a bearing capacity of footing subjected to centric vertical load and placed at a certain depth. A reduction factor has been proposed to estimate the variation of the bearing capacity when the model footing is exposed to eccentrically inclined load and the degree of reduction with respect to the reference case ($e=0$, $\alpha=0$) at similar embedment ratio.

It can be noted that, the embedment ratio has a significant effect on the bearing capacity of model footing at different values of the eccentricity and inclination. All curves nearly trend to have the same behavior when the footing is loaded under eccentrically inclined loads. According to calculations which have been carried out to assess the decrease of bearing capacity using RF, the magnitude of reduction in the bearing capacity starts to increase with the increase of eccentricity ratio.

Also, in general speaking, the reduction factor is decreased as the depth where the model footing placed is increased especially for the case of load inclination of (10°) and thereafter to (20°). Details of the reduction factor of the model footing at different conditions are displayed in **Table 2**. It is found that, the decreasing of bearing capacity is raised as the eccentricity and the inclination angles are increased. As well as, attaining from the ($\alpha=10$), the reduction factor at an eccentricity ratio of (0.15) is converted from (63.8 to 49.3%) when the embedment ratio increased from (0 to 1), and for the same ratio, the reduction factor is varied from (73.0 to 61.2%) and (82.9 to 65.6%) when the load is applied at an angles of (15° and 20°) respectively.

This state can be justified to placing the model footing at a certain depth will increase the bearing capacity by reducing the ability of model footing to slide or to overturn due to the eccentric inclined load. Therefore, presence of the footing below the ground level can minimize these effects by the increase of base resistance to the horizontal forces and reduce the upheaval of soil at the side of footing where the point of load is applied at which the model will be supported by stronger region. Consequently, the amount of decreasing in the bearing capacity or by other words the reduction factor is decreased.

5. CONCLUSIONS

Based on the results of this investigation, the following main conclusions can be drawn:

1. Bearing capacity of model footing is separately reduced with both of the inclination angle (α) and eccentricity ratio (e/B), and this effect appears largely when the model footing is exposed to eccentrically inclined load directly.
2. A pronounced influence of the inclination angle on the ultimate capacity of footing presents that, the footing capacity is decreased by (8, 31, 51 and 70%) for ($\alpha=5^\circ$, 10° , 15° and 20°) respectively and at $D_f/B=0$ and $e/B=0$. For the case of $D_f/B=0.5$ and $e/B=0$, the ultimate capacity is minimized by (8, 25, 39 and 58%) for $D_f/B=0.5$ and $e/B=0$. Also, the footing capacity is reduced by (9, 30, 50 and 57%) for the case of $D_f/B=1$ and $e/B=0$.
3. The increase of mobilized moment ($M= v. e$) was obtained about (80 to 136%) at maximum eccentricity ratio (0.15) and embedment ratio of (0.5 to 1.0) respectively, as compared with the surface footing case.
4. The reduction factor (RF) trends to decrease as the embedment ratio increases, and decrease significantly with the eccentricity ratio and inclination angle.
5. The effects of sliding and overturning due to eccentric inclined load are minimized when the model footing is placed at a certain depth below ground level.

**REFERENCES**

- Atalar, C., Patra C.R., Das B.M., and Sivakugan N., 2013, *Bearing Capacity of Shallow Foundation Under Eccentrically Inclined Load*, Proceedings of the 18th International Conference on Soil Mechanics and Geotechnical Engineering, Paris.
- Bransby, M.F., and Randolph, M.F., 1998, *Combined Loading of Skirted Foundations*, *Geotechnique*, vol. 48, issue (5), PP. 637–655.
- Gottardi, G., and Butterfield, R., 1993, *on The Bearing Capacity of Surface Footings on Sand Under General Planar Loads*, *Soils and Foundations*, vol. 33, issue (3), PP. 68–79.
- Loukidis D., Chakraborty T., and Salgado R., 2008, *Bearing Capacity of Strip Footings on Purely Frictional Soil Under Eccentric and Inclined Loads*, *Canadian Geotechnical Journal*, vol. 45, PP. 768-787.
- Pritam D., Soumya, R., and Bikash, C.C., 2013, *Behavior of Rigid Footing Under Inclined and Eccentric Loading*, *Journal of Annals of Pure and Applied Mathematics*, Vol. 5, issue (1), PP. 71-81.
- Purkayastha, R.D. and Char, R.A.N., 1977, *Stability Analysis for Eccentrically Loaded Footings*, *Journal of the Geotechnical Engineering Division, ASCE*, vol. 103, issue (6), PP. 647-651.
- Saran, S. and Agarwal, R.K., 1991, *Bearing Capacity of Eccentrically Oblique Loaded Foundation*, *Journal of Geotechnical Engineering, ASCE*, vol.117, issue (11), PP. 1669-1690.
- Murthy, V.N.S., 2002, *Principles and Practices of Soil Mechanics and Foundation Engineering*, Marcel Dekker Inc., New York.

NOMENCLATURE

B and B' = actual and effective footing width, m.

C_u = cohesion of soil, kPa.

D_f = excavated footing depth, m.

D_f/B = embedment ratio, dimensionless.

E_s = modulus of elasticity, kPa.

e = eccentricity, m.

e/B = eccentricity ratio, dimensionless.

H = horizontal resistance of footing, kN.

M = applied moment, kN.m.

N_q and N_γ = bearing capacity factors, dimensionless.

P_p = passive force of soil, kN.

RF = reduction factor in bearing capacity, dimensionless.

R_{int} = interface reduction factor, dimensionless.

R^2 = coefficient of regression, dimensionless.

V = vertical applied load, kN.

α = inclination angle, degree.

γ = unit weight of soil, kN/m^3 .
 δ = angle of wall friction, degree.
 ϕ = angle of internal friction, degree.
 ψ = angle of dilation, degree.

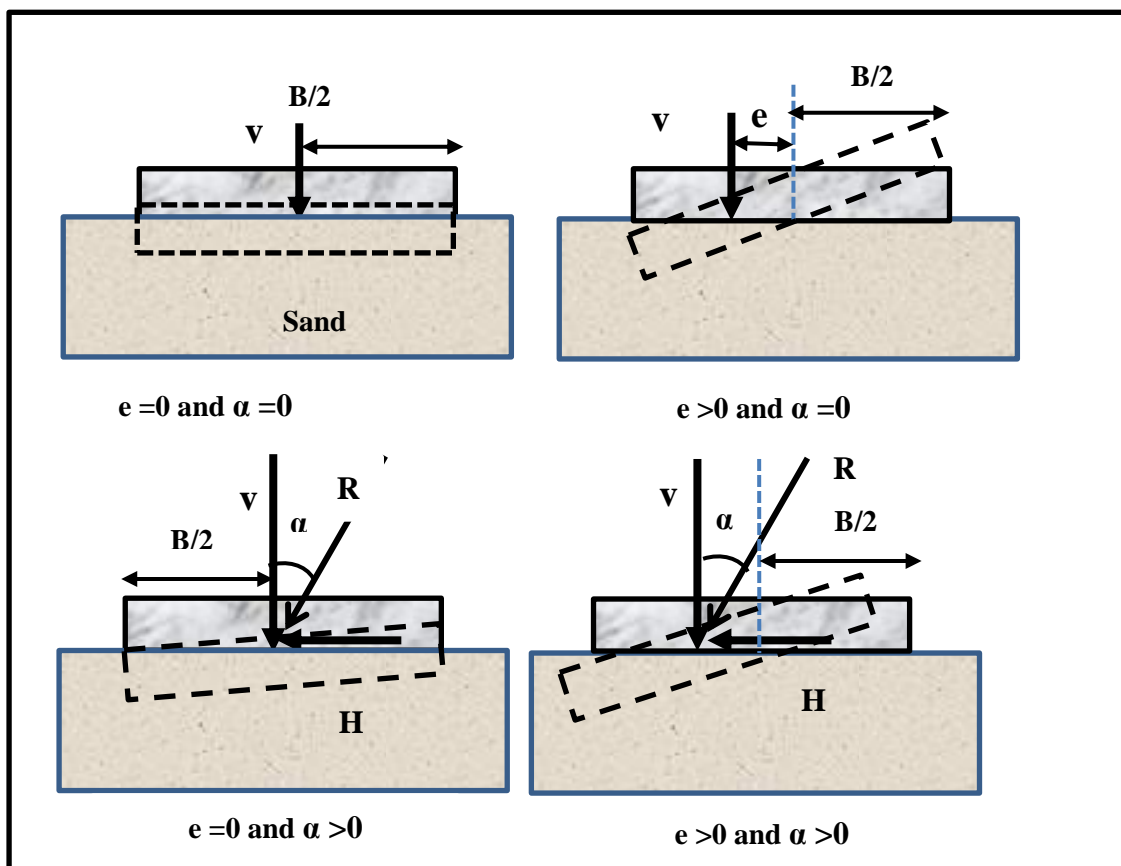


Figure 1. Footing loading condition where R, V and H are resultant, vertical and horizontal loads respectively.

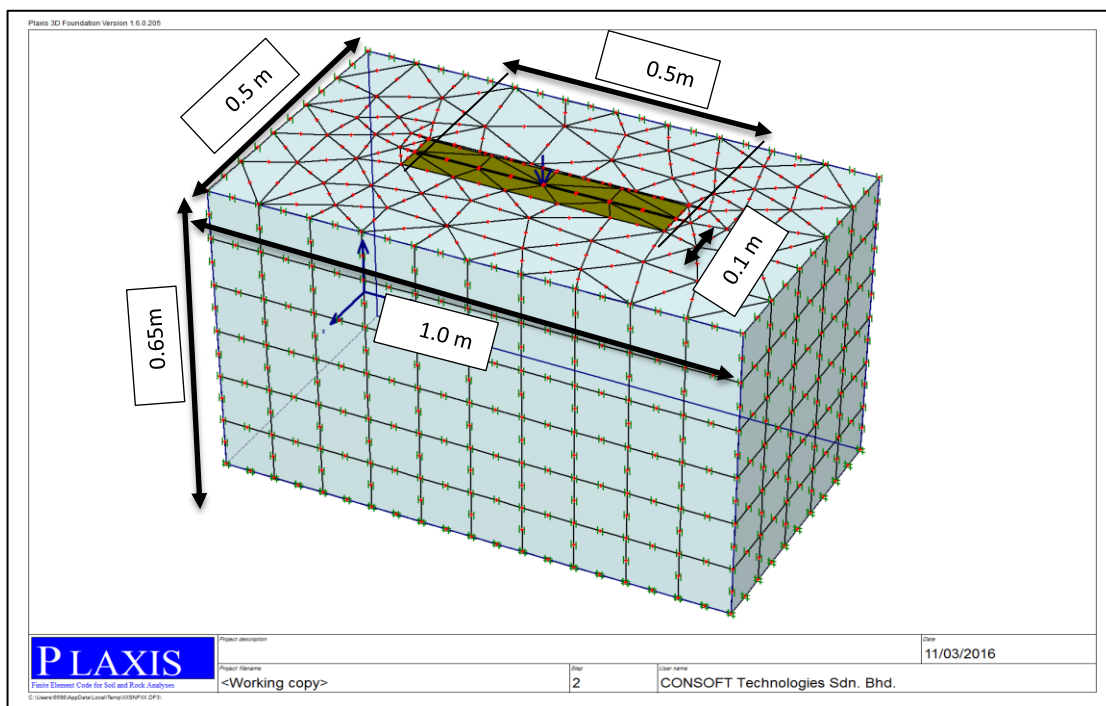


Figure 2a. Geometry of mesh boundary when footing is installed at $D_f/B=0$

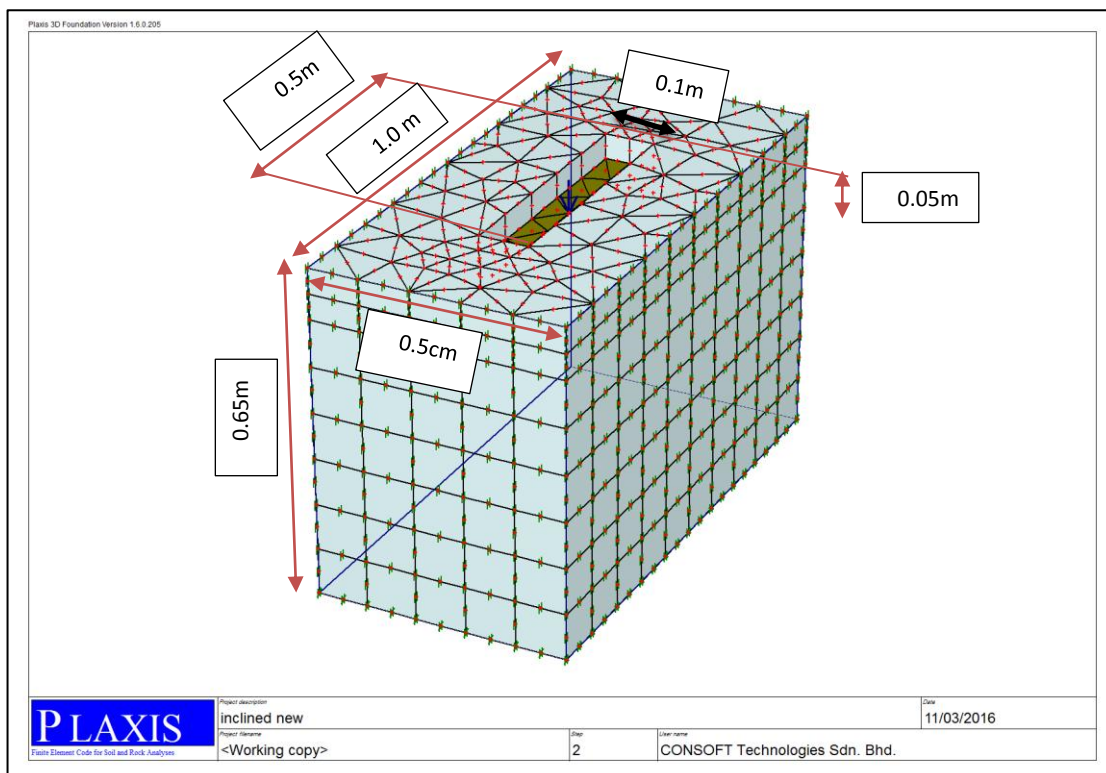


Figure 2b. Geometry of mesh boundary when footing is installed at $D_f/B=0.5$

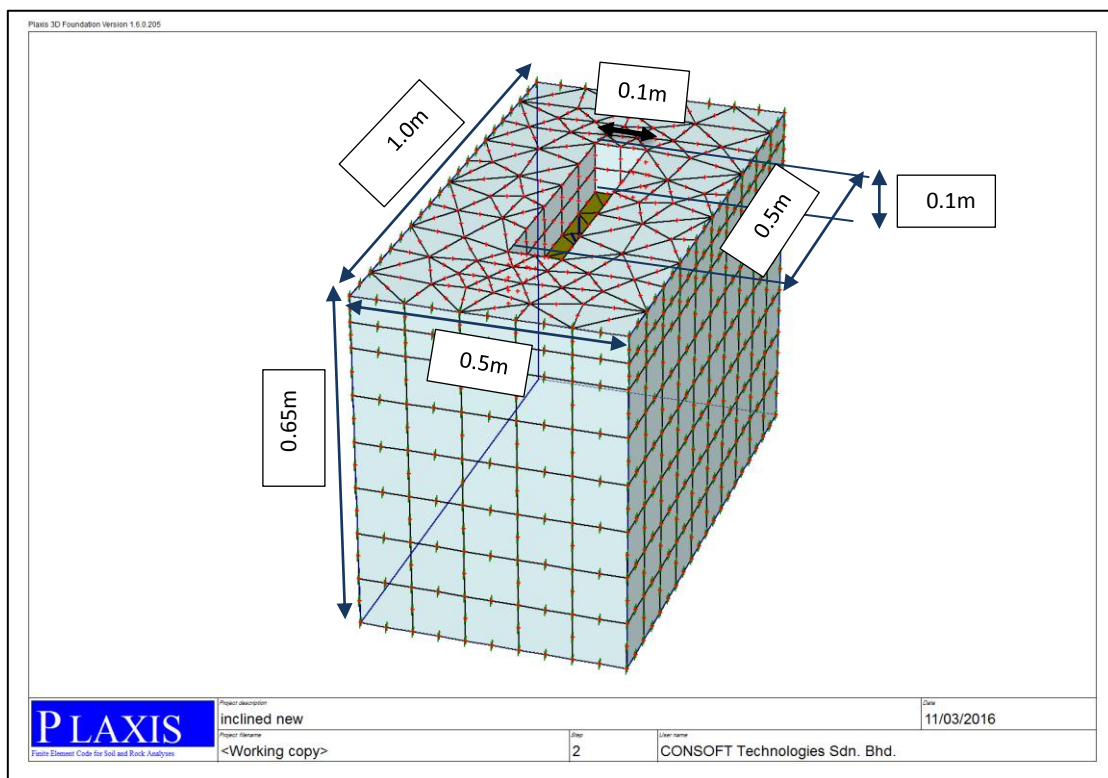


Figure 2c. Geometry of mesh boundary when footing is installed at A) $D_f/B=1$

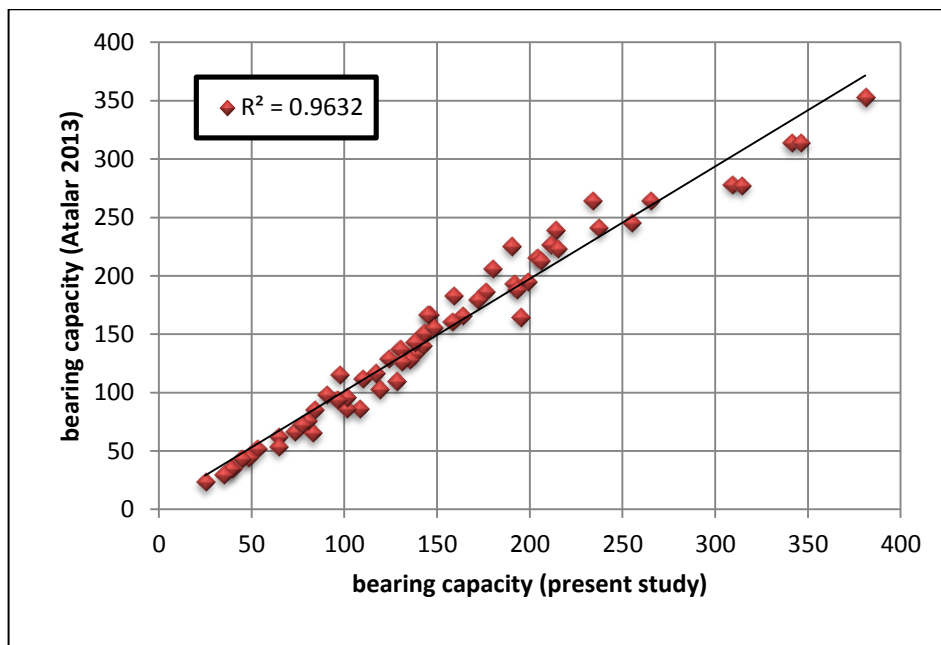


Figure 3. Comparison between bearing capacity values for present and previous studies.

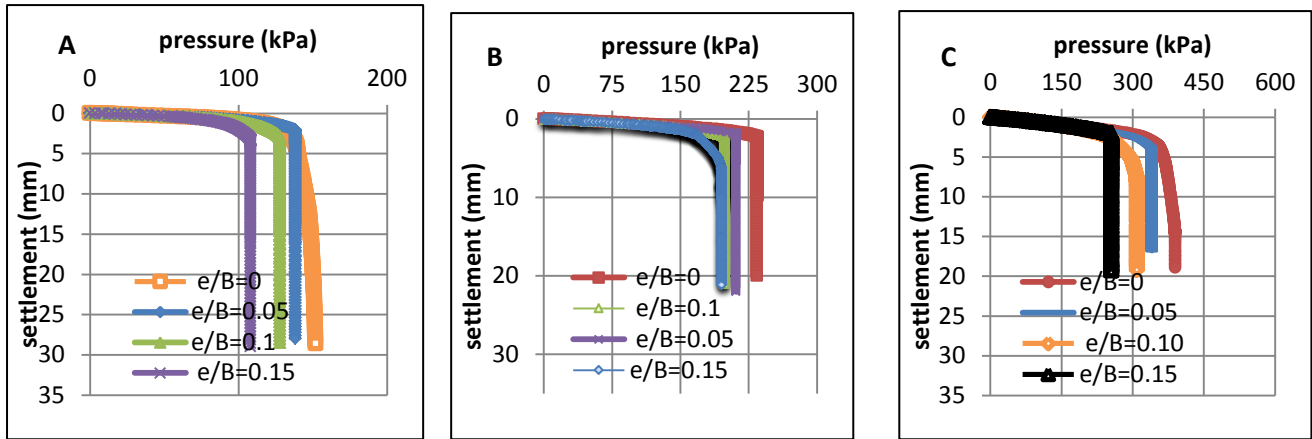


Figure 4. Pressure-settlement relationship of eccentrically vertical loaded model footing at values of embedment ratio of A) $D_f/B = 0$, B) $D_f/B = 0.5$ and C) $D_f/B = 1.0$.

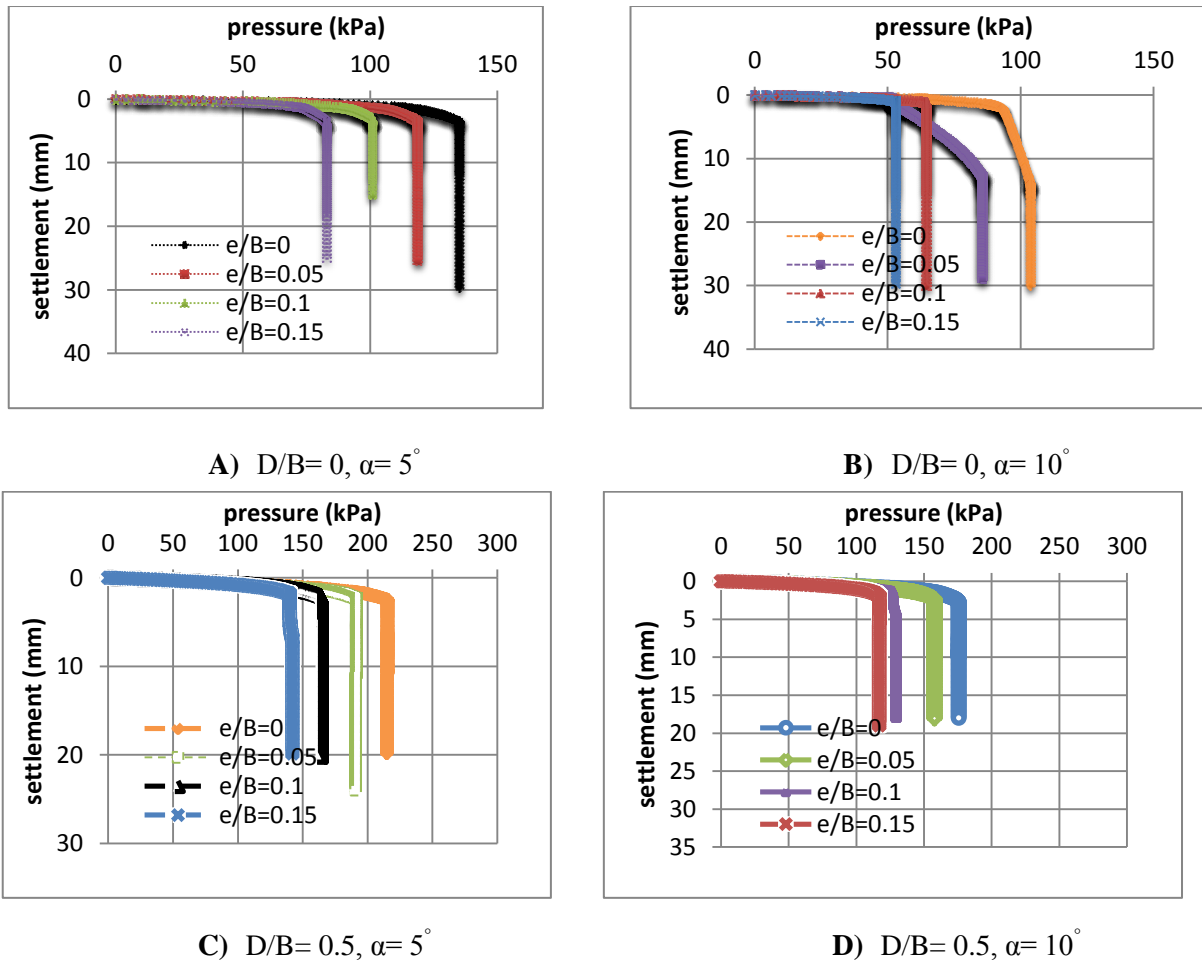
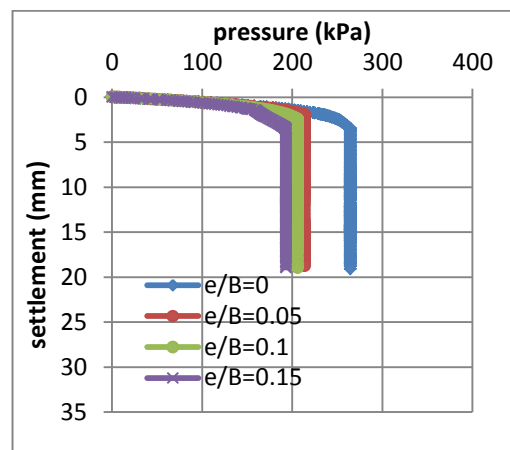
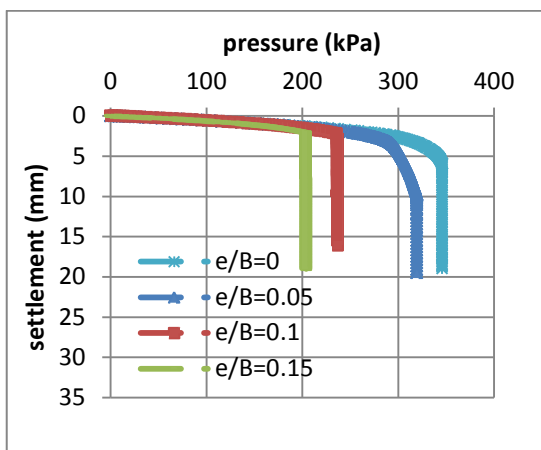
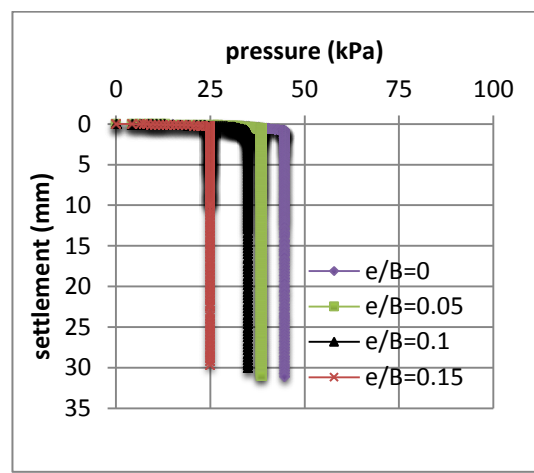
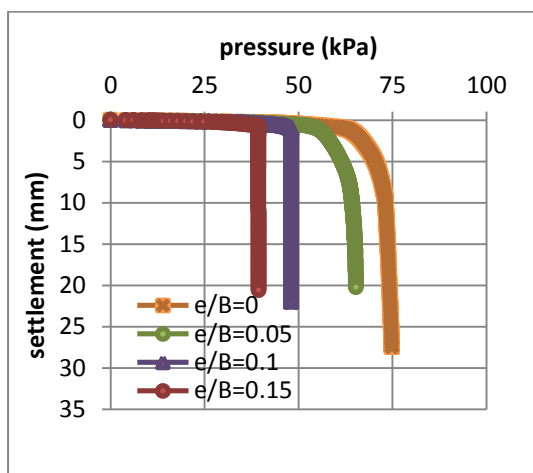


Figure 5. Stress- settlement curves for all models that have been analyzed at different conditions of loading.



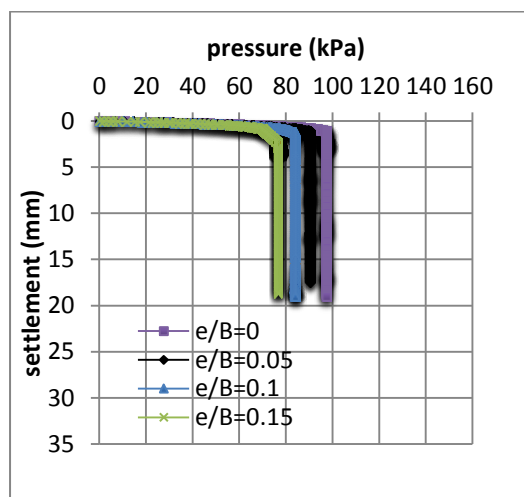
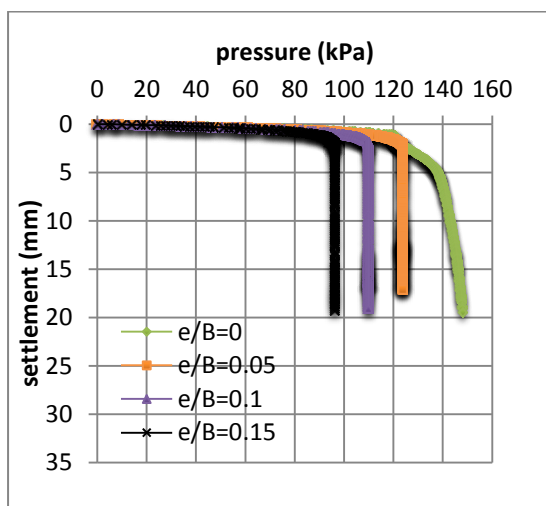
E) $D/B=1.0, \alpha=5^\circ$

F) $D/B=1.0, \alpha=10^\circ$



G) $D/B=0, \alpha=15^\circ$

H) $D/B=0, \alpha=20^\circ$



I) $D/B=0.5, \alpha=15^\circ$

J) $D/B=0.5, \alpha=20^\circ$

Figure 5. Continue.

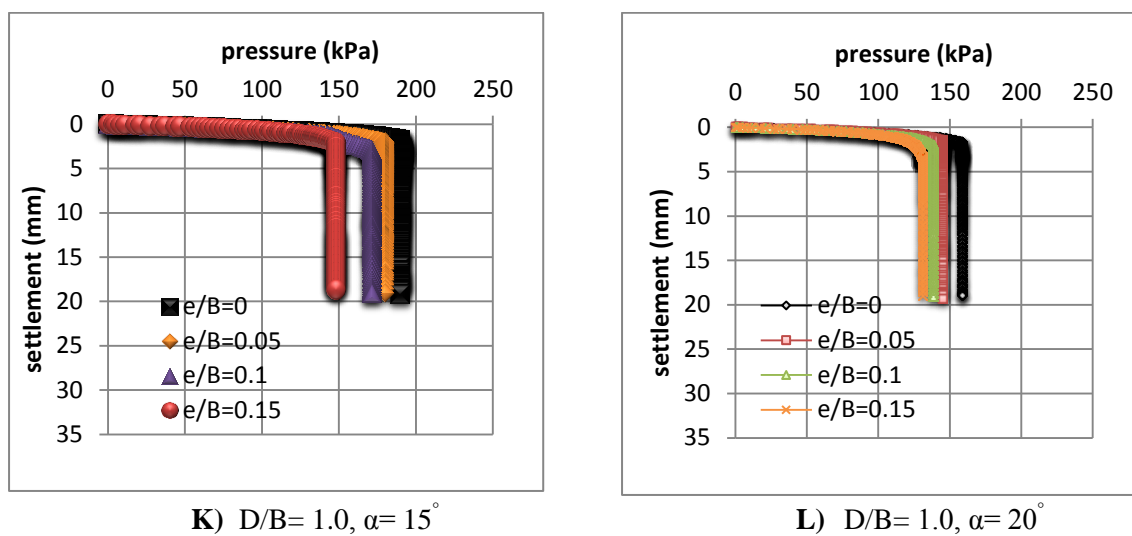


Figure 5. Continue.

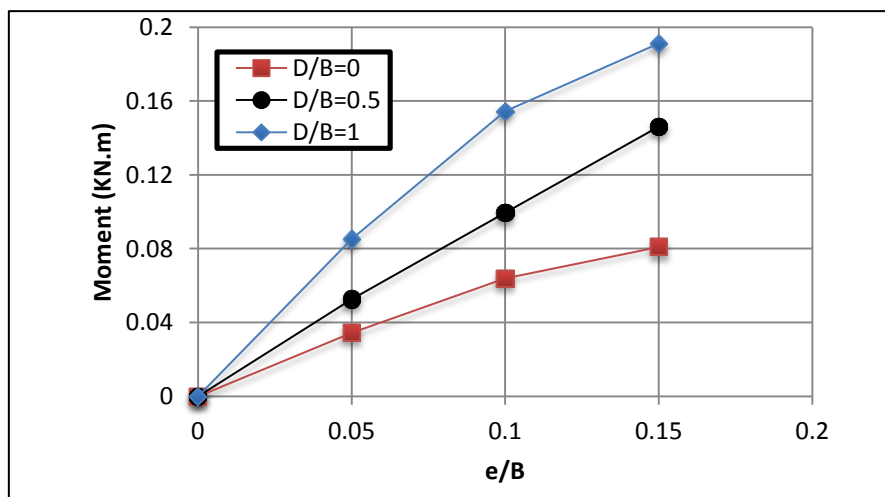
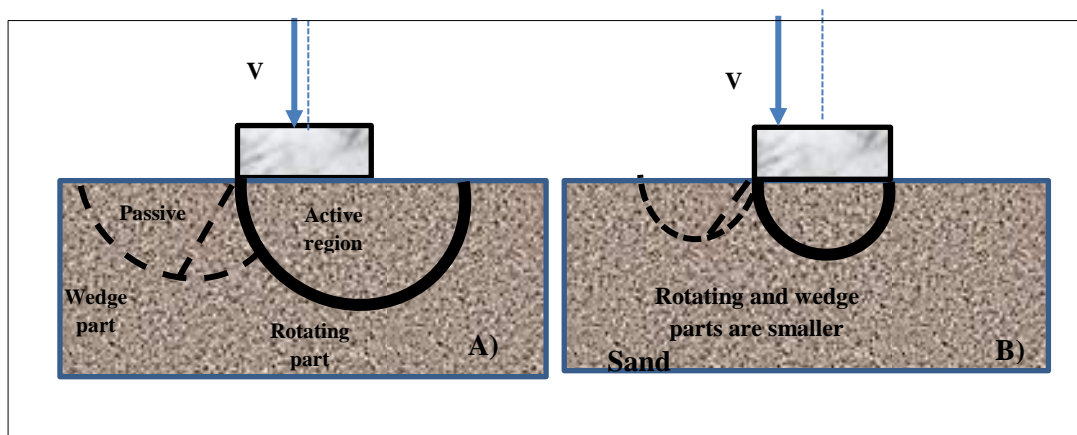


Figure 6. Maximum moment vs. eccentricity ratio relationship of vertically eccentric footing.

Figure 7. Mechanism of failure of eccentric vertical loaded footing A) $e < B/6$ and B) $e > B/6$.

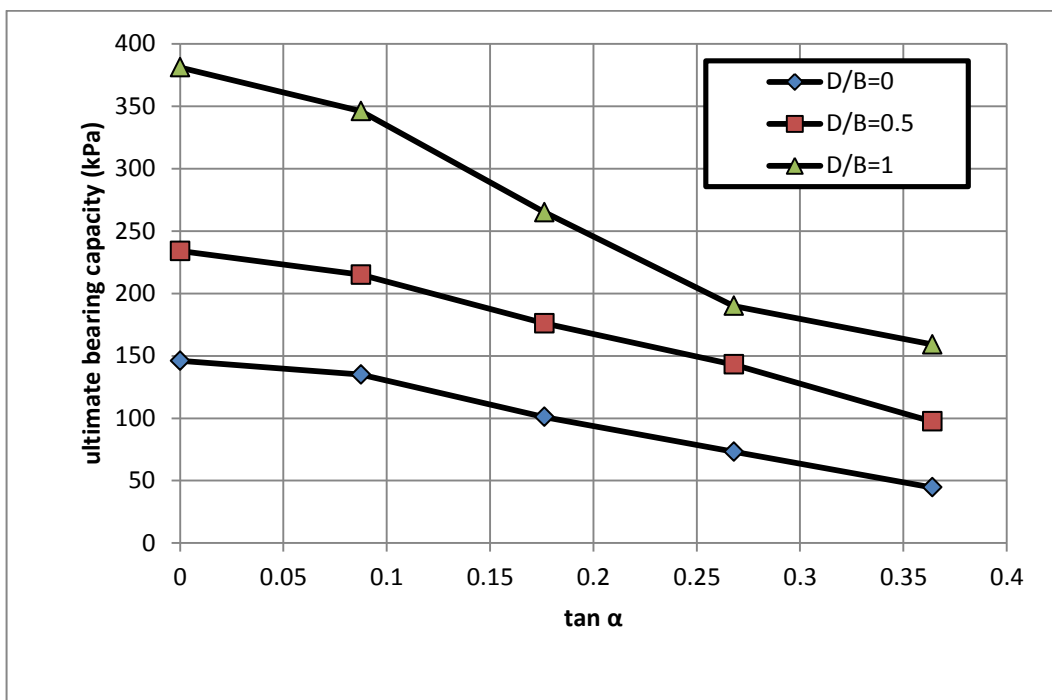


Figure 8. Effect of load inclination on the bearing capacity at different embedment ratio.

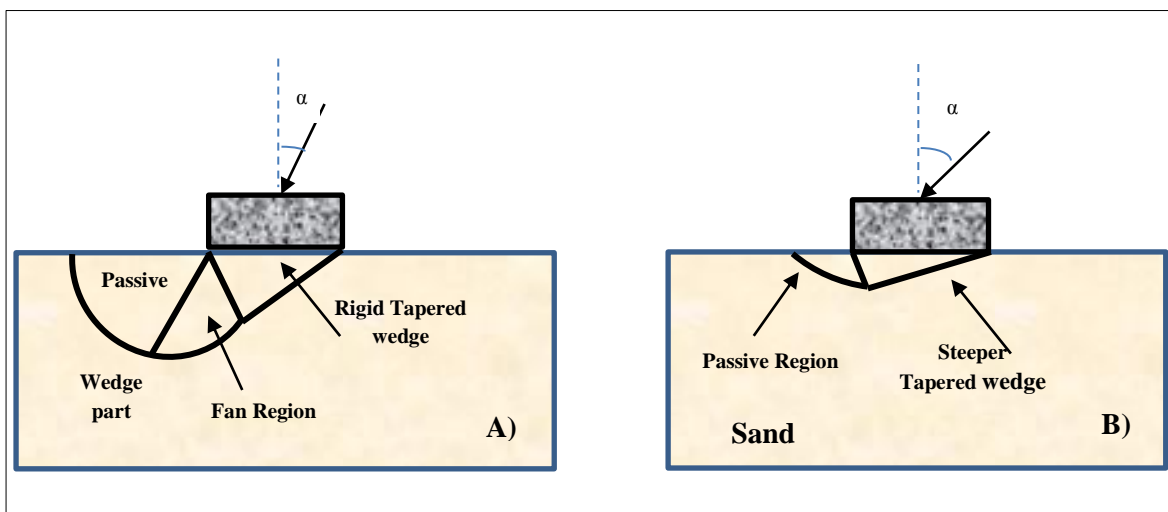


Figure 9. Mechanism of failure of centric inclined loaded footing A) $\alpha = 10^\circ$ and B) $\alpha = 20^\circ$.

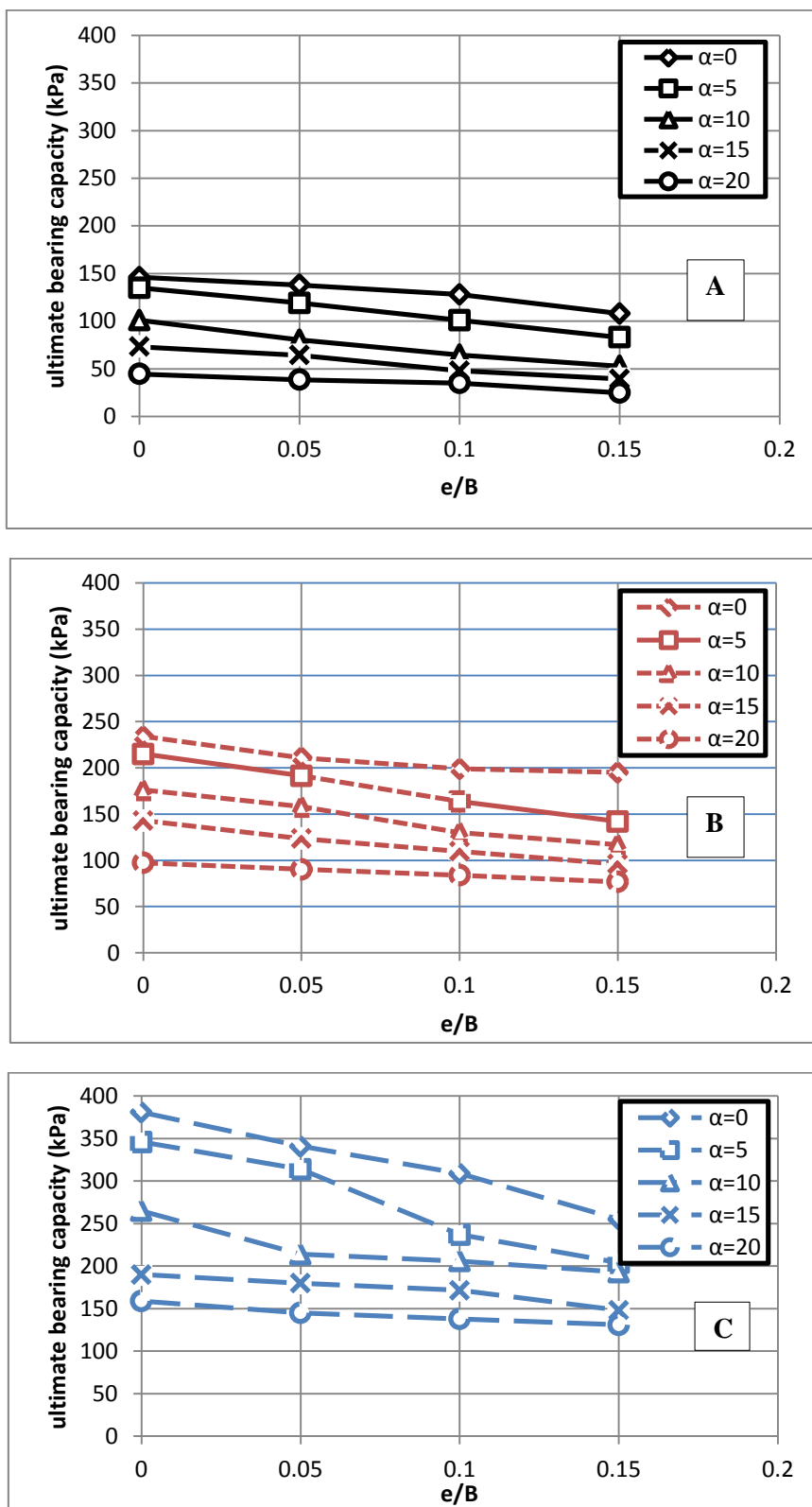


Figure 10. Effect of inclination angle and eccentricity ratio on the bearing capacity of model footing at different embedment ratios A) $D_f/B = 0$, B) $D_f/B = 0.5$ and C) $D_f/B = 1.0$.

**Table 1.** Parameters of soil model adopted in present study.

parameter	Index
Type of Material	Sand
Material Model	Mohr coulomb
Modulus of elasticity E_s (kN/m ²)	36000
Poisson's ratio, ν	0.30
Angles of internal friction ϕ	41°
Angle of Dilatancy ψ	11°
Cohesion C_u (kN/m ²)	0.001
Dry unit weight γ (kN/m ³)	14.36
Interface reduction factor R_{int}	0.8
Stiffness of footing material (kN/m ²)	65000000

Table 2. Reduction factor and bearing capacities obtained from the present and previous studies at different cases.

No.	D_f/B	α	e/B	q_u (present study) (kPa) (1)	q_u (Atalar. et. al., 2013) (kPa) (2)	(Col.1-co12)/col.2 Deviation (3)	(RF) %
1	0	0	0	146	166.77	-12.45	0
2	0	0	0.05	138	133.42	3.43	5.5
3	0	0	0.1	128	109.87	16.50	12.3
4	0	0	0.15	108	86.33	25.10	26
5	0	5	0	135	128.51	5.05	7.5
6	0	5	0.05	119	103.01	15.52	18.5
7	0	5	0.1	101	86.33	16.99	30.8
8	0	5	0.15	83	65.73	26.27	43.2
9	0	10	0	101	96.14	5.06	30.8
10	0	10	0.05	80.4	76.52	5.07	44.9
11	0	10	0.1	64.6	62.78	2.89	55.8
12	0	10	0.15	52.9	51.99	1.75	63.8
13	0	15	0	73.2	66.71	9.72	49.9
14	0	15	0.05	64.3	53.96	19.16	56
15	0	15	0.1	48	44.15	8.72	67.1
16	0	15	0.15	39.4	35.12	12.18	73
17	0	20	0	44.6	43.16	3.33	69.5
18	0	20	0.05	38.5	34.83	10.53	73.6
19	0	20	0.1	35	29.43	18.92	76.02
20	0	20	0.15	24.9	23.54	5.77	82.9
21	0.5	0	0	234	264.87	-11.65	0
22	0.5	0	0.05	211	226.61	-6.88	9.8
23	0.5	0	0.1	199	195.22	1.93	15
24	0.5	0	0.15	195	164.81	18.31	16.7
25	0.5	5	0	215	223.67	-3.87	8.1
26	0.5	5	0.05	191.5	193.26	-0.91	18.2
27	0.5	5	0.1	163.8	165.79	-1.20	30
28	0.5	5	0.15	142	140.28	1.22	39
29	0.5	10	0	176	186.39	-5.57	24.8
30	0.5	10	0.05	158	160.88	-1.79	32.5
31	0.5	10	0.1	130	137.34	-5.34	44.4
32	0.5	10	0.15	117	116.74	0.22	50
33	0.5	15	0	143	151.07	-5.34	38.9
34	0.5	15	0.05	123.6	129.49	-4.54	47.2



35	0.5	15	0.1	109.8	111.83	-1.81	53.1
36	0.5	15	0.15	96	94.18	1.93	59
37	0.5	20	0	97.4	115.76	-15.86	58.4
38	0.5	20	0.05	90.3	98.1	-7.95	61.4
39	0.5	20	0.1	84	85.35	-1.58	64.1
40	0.5	20	0.15	76.8	72.59	5.79	67.2
41	1	0	0	381	353.16	7.88	0
42	1	0	0.05	341	313.92	8.62	10.5
43	1	0	0.1	309	278.6	10.91	18.9
44	1	0	0.15	255	245.25	3.97	33.1
45	1	5	0	346	313.92	10.21	9.2
46	1	5	0.05	320	277.62	15.26	17.6
47	1	5	0.1	237	241.33	-1.79	37.8
48	1	5	0.15	204	215.82	-5.47	46.5
49	1	10	0	265	264.87	0.04	30.4
50	1	10	0.05	214	239.36	-10.59	43.8
51	1	10	0.1	206	212.88	-3.23	45.9
52	1	10	0.15	193	188.35	2.46	49.3
53	1	15	0	190	225.63	-15.79	50.13
54	1	15	0.05	180	206.01	-12.62	52.8
55	1	15	0.1	171.6	179.52	-4.41	55
56	1	15	0.15	148	155.98	-5.11	61.2
57	1	20	0	159	183.45	-13.32	58.2
58	1	20	0.05	145	166.77	-13.05	61.9
59	1	20	0.1	138	143.23	-3.65	63.8
60	1	20	0.15	131	126.55	3.51	65.6
						$\Sigma \text{value} =7.65\%$ $=0.9235$	